Early Alveolar Epithelial Dysfunction Promotes Lung Inflammation in a Mouse Model of Hermansky-Pudlak Syndrome

Elena N. Atochina-Vasserman[1], Sandra R. Bates[2], Peggy Zhang[3], Helen Abramova[1,5], Zhenguo Zhang[3], Linda Gonzales[3], Jian-Qin Tao[2], Bernadette R. Gochuico[4], William Gahl[4], Chang-Jiang Guo[5], Andrew J. Gow[5], Michael F. Beers[1], and Susan Guttentag[3]

[1]Division of Pulmonary and Critical Care Medicine and [2]Institute for Environmental Medicine, University of Pennsylvania School of Medicine, and [3]Division of Neonatology, Department of Pediatrics, Children's Hospital of Philadelphia, Philadelphia, Pennsylvania [4]Section on Human Biochemical Genetics, Medical Genetics Branch, National Human Genome Research Institute, National Institutes of Health, Bethesda, Maryland; and [5]Department of Pharmacology, Ernest Mario School of Pharmacy, Rutgers University, Piscataway, New Jersey

Rationale: **The pulmonary phenotype of Hermansky-Pudlak syndrome (HPS) in adults includes foamy alveolar type 2 cells, inflammation, and lung remodeling, but there is no information about ontogeny or early disease mediators.**

Objectives: **To establish the ontogeny of HPS lung disease in an animal model, examine disease mediators, and relate them to patients with HPS1.**

Methods: **Mice with mutations in both HPS1/pale ear and HPS2/*AP3B1*/pearl (EPPE mice) were studied longitudinally. Total lung homogenate, lung tissue sections, and bronchoalveolar lavage (BAL) were examined for phospholipid, collagen, histology, cell counts, chemokines, surfactant protein D (SP-D), and S-nitrosylated SP-D. Isolated alveolar epithelial cells were examined for expression of inflammatory mediators, and chemotaxis assays were used to assess their importance. Pulmonary function test results and BAL from patients with HPS1 and normal volunteers were examined for clinical correlation.**

Measurements and Main Results: **EPPE mice develop increased total lung phospholipid, followed by a macrophage-predominant pulmonary inflammation, and lung remodeling including fibrosis. BAL fluid from EPPE animals exhibited early accumulation of both SP-D and S-nitrosylated SP-D. BAL fluid from patients with HPS1 exhibited similar changes in SP-D that correlated inversely with pulmonary function. Alveolar epithelial cells demonstrated expression of both monocyte chemotactic protein (MCP)-1 and inducible nitric oxide synthase in juvenile EPPE mice. Last, BAL from EPPE mice and patients with HPS1 enhanced migration of RAW267.4 cells, which was attenuated by immunodepletion of SP-D and MCP-1.**

Conclusions: **Inflammation is initiated from the abnormal alveolar epithelial cells in HPS, and S-nitrosylated SP-D plays a significant role in amplifying pulmonary inflammation.**

Keywords: Hermansky-Pudlak syndrome; S-nitrosylation; surfactant protein D; lung remodeling

AT A GLANCE COMMENTARY

Scientific Knowledge on the Subject

The development of clinically significant lung disease in adult patients with Hermansky-Pudlak syndrome (HPS) is becoming increasingly recognized.

What This Study Adds to the Field

Using HPS mouse models, this data establishes that alveolar epithelial cell dysfunction initiates inflammation early in HPS, providing a rationale for the development of novel therapies and justification for more detailed examination of pediatric patients with HPS.

Hermansky-Pudlak syndrome (HPS) is a group of genetic disorders recognizable by the combination of clinical findings of oculocutaneous albinism, platelet dysfunction, and in some cases progressive pulmonary fibrosis and/or granulomatous colitis (1). Of the eight clinical subtypes of HPS, only HPS1, HPS2 (2), and HPS4 are known to be associated with pulmonary fibrosis. The genes responsible for HPS, except for HPS2, have no established function; the HPS2 gene is *AP3B1*, a subunit of the AP-3 complex responsible for intracellular membrane trafficking. HPS proteins participate in heteropolymeric complexes (called BLOCS, for biogenesis of lysosome-like organelle complexes), but the precise functions of these complexes remain unclear (1). BLOCs are ubiquitously expressed but play critical roles in specialized lysosome-like organelles, such as melanosomes and platelet dense granules. Thus, defective melanosome biogenesis in melanocytes accounts for the oculocutaneous albinism, and defective platelet dense granule formation accounts for the bleeding disorders in patients with HPS.

Alveolar type 2 cells also contain a lysosome-like secretory organelle. The surfactant-containing lamellar body exhibits an acidic pH, undergoes regulated secretion, and possesses lysosomal transmembrane proteins in the limiting membrane, notably Lamp1 and Lamp3. Autopsy studies of adults with HPS have demonstrated foamy degeneration of alveolar type 2 cells as well as hyperplasia, alveolar inflammation, and pulmonary fibrosis (3). Mouse models of HPS, including the mouse homologs of HPS1 (pale ear) and HPS2 (pearl), similarly display foamy degeneration of alveolar type 2 cells of adult animals. Adult pale ear and pearl animals exhibit a macrophage-predominant alveolar inflammation (4, 5) and develop emphysema with aging but do not develop pulmonary fibrosis unless exposed to fibrogenic stimuli such as bleomycin, albeit at much lower doses than for littermate

(*Received in original form November 22, 2010; accepted in final form May 24, 2011*)

Supported by the Intramural Research Program of the National Human Genome Research Institute, National Institutes of Health (B.R.G., W.G.), and by extramural funding from the National Institutes of Health through HL086621 (A.J.G.), HL019737 (S.R.B., M.F.B.), HL064520 (M.F.B.), ES013508 (M.F.B.), and HL059959 (S.G.).

Author contributions: Conception and design: S.G., M.F.B.; acquisition of data: E.N.A.-V., S.R.B., P.Z., H.A., Z.Z., L.G., J.-Q.T., B.R.G., W.G., C.-J.G.; analysis and interpretation: E.N.A.-V., C.-J.G., A.J.G., M.F.B., S.G.; drafting the manuscript for important intellectual content: all; final approval: all.

Correspondence and requests for reprints should be addressed to Susan Guttentag, M.D., 416G Abramson Research Center, 3615 Civic Center Blvd., Philadelphia, PA 19104. E-mail: guttentag@email.chop.edu

This article has an online supplement, which is available from this issue's table of contents at www.atsjournals.org

Am J Respir Crit Care Med Vol 184. pp 449–458, 2011
Originally Published in Press as DOI: 10.1164/rccm.201011-1882OC on May 26, 2011
Internet address: www.atsjournals.org

controls (6). Intercrossing HPS1/pale ear and HPS2/pearl strains results in a more severe phenotype (4) that more closely resembles the pulmonary manifestations of human HPS. Adult pale ear/pearl doubly homozygous (EPPE) mice exhibit foamy alveolar type 2 cells associated with defective surfactant secretion (7), macrophage-predominant alveolar inflammation, and lung remodeling most notable for tissue destruction (4). Older animals have been shown also to exhibit epithelial cell apoptosis and spontaneous pulmonary fibrosis (8).

To better understand the pathogenesis of HPS lung disease, we have performed a detailed longitudinal analysis of pale ear, pearl, and EPPE mice over 32 weeks of age. Whereas the single mutations result in modest changes in phospholipid accumulation and inflammatory cell infiltration, the doubly homozygous animals exhibit a more severe phenotype than is explainable by the single mutations alone. We demonstrate that intracellular phospholipid accumulation within alveolar type 2 cells of EPPE mice is an early event, and precedes the influx of macrophages into the alveolar space. We show that alveolar inflammation is temporally associated with the appearance and increase in both the monocyte/macrophage chemokine monocyte chemotactic protein (MCP)-1 as well as S-nitrosylated surfactant protein D (SNO-SP-D), itself a potent stimulus for alveolar inflammation and macrophage chemotaxis (9). Mechanistically, we define the alveolar type 2 cell in HPS mice as the source of both MCP-1 and nitric oxide, which contribute to the development of the observed inflammation and the formation of SNO-SP-D. Importantly, we also show that S-nitrosylated SP-D is increased in humans with HPS1 and correlates with disease severity. Last, as proof of principle, the proinflammatory effects of bronchoalveolar lavage (BAL) from both EPPE mice and humans with HPS1 on macrophage migration were mitigated by immunodepletion of these two keys mediators, SNO-SP-D and MCP-1. Together, these data suggest that early, progressive dysregulation of alveolar epithelial homeostasis is a mechanism for chronic alveolar inflammation in Hermansky-Pudlak syndrome.

A portion of the results of this study has been previously reported in the form of an abstract (10).

METHODS

Complete and detailed methods can be found in the online supplement.

Animals

Wild-type C57BL/6J mice and mutant *Hps1*^{ep}/*Hps1*^{ep}, *Ap3b1*^{pe}/*Ap3b1*^{pe} (EPPE) mice on the same C57BL/6J background were maintained and bred at the Laboratory Animal Facility in the Abramson Research Center at the Children's Hospital Research Institute of the Children's Hospital of Philadelphia (Philadelphia, PA). All animal protocols were reviewed and approved by the Institutional Animal Care and Use Committees and adhered to the principles of the National Institutes of Health *Guide for the Care and Use of Laboratory Animals*.

Alveolar Epithelial Cell Isolation

Isolated primary alveolar epithelial cells from wild-type (WT) and EPPE animals were cultured in the presence or absence of brefeldin A (10 μg/ml; Sigma, Inc., St. Louis, MO) for 4 hours. Cells were then either used to isolate RNA or were fixed in 4% paraformaldehyde for 1 hour for immunostaining.

Phospholipid Analysis of Lung Tissue Samples

A sample of the right upper lobe of mouse lung was homogenized in 500 μl of distilled water. Aliquots were analyzed for protein (11) and the lipids were extracted with chloroform–methanol (12) followed by phospholipid analysis (13).

Sircol Assay

Acid-soluble collagens in homogenates of frozen lung tissue were analyzed using the Sircol assay (Biocolor Ltd., Carrickfergus, UK).

Samples and Data from Patients with HPS

As previously described (14), subjects with HPS1 and healthy research volunteers were evaluated at the National Institutes of Health Clinical Center (Bethesda, MD) and were enrolled in protocols 95-HG-0193 and/or 04-H-0211, which were approved by the Institutional Review Boards of the National Human Genome Research Institute (Bethesda, MD).

Polyacrylamide Gel Electrophoresis and Immunoblotting

Total BAL SP-D was analyzed by denaturing sodium dodecyl sulfate–polyacrylamide gel electrophoresis, SP-D quaternary structure by native gel electrophoresis, and S-nitrosylated SP-D by the biotin-switch method as previously described (15).

Nitric Oxide Measurements

BAL samples were analyzed for nitric oxide (NO) metabolites by chemical reduction and chemiluminescence, using the Ionics/Sievers nitric oxide analyzer 280 (NOA 280; Ionics Instruments, Boulder, CO) as previously described (9).

Cytokine Analysis

Multiplex cytokine analysis was performed on samples of BAL (Endogen Searchlight; Pierce, Rockford, IL). For samples from animals greater than 2 weeks of age, each sample consisted of single animals. For animals not more than 2 weeks of age, samples were pooled from two to five animals as needed to meet the minimal volume requirements for the assay.

Chemotaxis Assay

Directed migration (chemotaxis) of cells was performed with Boyden chambers and RAW 264.7 cells as previously described (9).

Quantitative Real-Time Polymerase Chain Reaction

Total cellular RNA from BAL cells and epithelial cells was isolated with an RNeasy kit (Qiagen, Valencia, CA) and a singleplex polymerase chain reaction (PCR) strategy using an ABI Prism 7900 system (ABI, Foster City, CA) as described previously (16). The primer/probe sets used were as follows: Ccl2 Mm00441242_m1, Nos2 Mm00440485_m1, IL-12b Mm00434174_m1, 18s Hs99999901_s1. Results are depicted as relative quantities (RQ) of RNA after correcting for 18S to normalize for variability in loading followed by normalizing to an appropriate WT sample.

Statistical Analysis

Data analyses were performed with Prism 5.0a software for the Macintosh (GraphPad Software, San Diego, CA). Parametric data were analyzed by single or two-way analysis of variance, each employing Bonferonni's post-hoc test, and results are expressed as means ± standard error. In all cases a P value less than 0.05 was considered as significant.

RESULTS

Age-related Increases in Lung Tissue Phospholipid, Alveolar Macrophages, and Fibrosis in EPPE Mice

We examined the lungs of animals doubly homozygous for the pale ear (HPS1) and pearl (HPS2; AP3b1) mutations between 3 days postnatally and 32 weeks of age. Total phospholipids were measured in lung tissue after bronchoalveolar lavage (Figure 1A). Total lung tissue phospholipids were nearly doubled by 3 days of age in the EPPE animals. Lung phospholipid levels reached a plateau by 2 weeks of age and were nearly fivefold elevated over those of wild-type (WT) animals. Although total phospholipid levels were elevated in pale ear and pearl mice (34 and 47%, respectively, by 16 wk), these did not achieve statistical significance compared with WT animals.

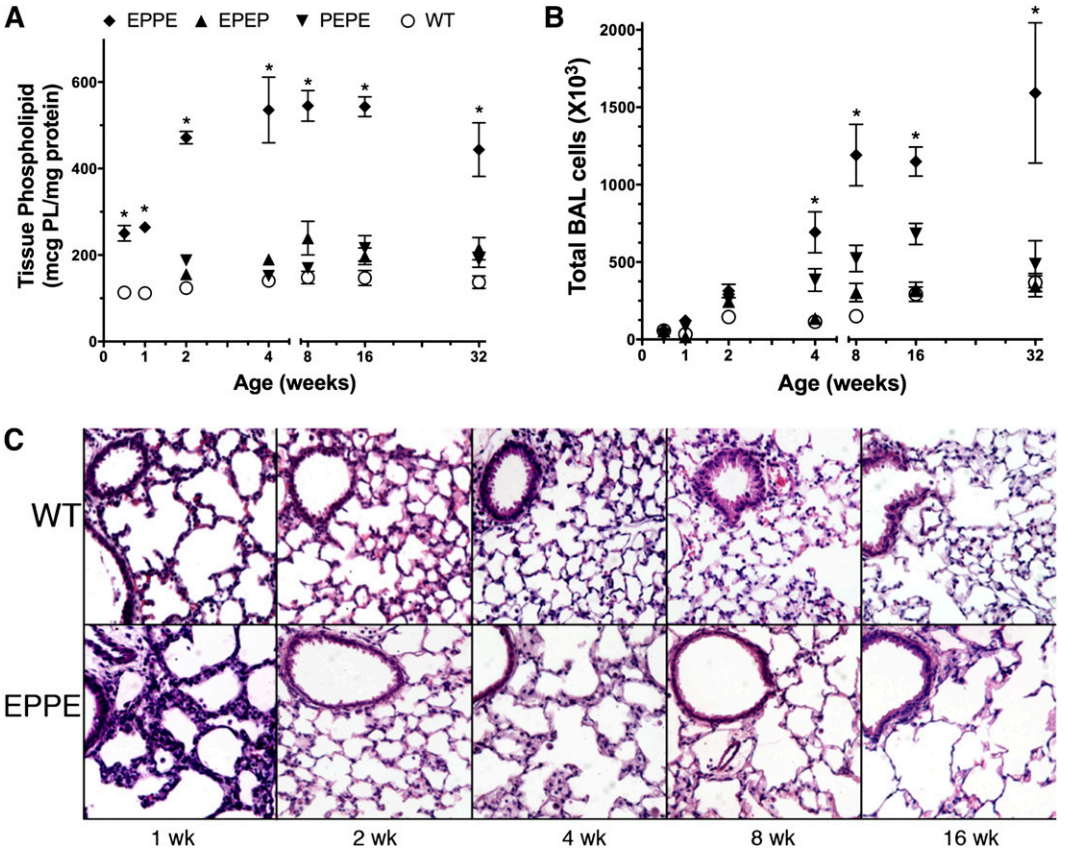

Figure 1. Ontogeny of phospholipid accumulation and inflammation in EPPE mice. Wild-type (WT), EPEP (pale ear), PEPE (pearl), and EPPE (pale ear/pearl) animals were examined at 3 days and 1, 2, 4, 8, 16, and 32 weeks of age. (*A*) Lung tissue phospholipid (micrograms of phospholipid [PL] per milligram of total protein) from three animals per time point (*$P < 0.01$ by two-way analysis of variance). (*B*) Total cell counts from bronchoalveolar lavage (BAL; n = 5–13 animals per time point; *$P < 0.01$). (*C*) WT and EPPE lungs were examined after inflation fixation, paraffin sectioning, and hematoxylin and eosin staining (n = 3 animals per age, genotype). Shown is a representative set of photomicrographs from 1- to 32-week WT and EPPE animals at an original magnification of ×20.

Complete bronchoalveolar lavage was performed on animals and cell counts were obtained from single animals. WT animals demonstrated increasing total BAL cells with age over the entire 32-week period (Figure 1B). A similar increase was seen in singly homozygous pale ear and pearl animals, with modest elevations compared with WT animals that did not achieve statistical significance. The EPPE mice had a significant, progressive increase in total BAL cells beginning after 2 weeks of age. BAL cells consisted of predominantly macrophages in all animals, with no significant differences between the percentages of macrophages, neutrophils, and lymphocytes among genotypes (data not shown).

To relate phospholipid content and BAL cell counts to the pulmonary phenotype in the mouse model, we inflation-fixed lungs *in situ* after bronchoalveolar lavage of animals between 1 and 32 weeks postnatal age, and stained serial paraffin sections with either hematoxylin and eosin, or trichrome. Lungs from EPPE animals were notable for hyperplasia of foamy type 2 cells that were foamy in appearance and increasing tissue destruction (Figure 1C) as previously described by others using this model (4). Only lungs from EPPE animals at 32 weeks displayed increased trichrome staining compared with WT animals (Figure 2A) as previously described by others (17). Increased fibrosis in EPPE mice was confirmed by the finding of elevated soluble collagen in the total lung homogenate only at 32 weeks (Figure 2B).

Early-onset Inflammation in EPPE Animals Is Associated with Increasing Amounts of SP-D and S-nitrosylated SP-D

SP-D, an important immunomodulator in the alveolus (15, 18–21), was increased in the BAL fluid of EPPE animals (Figure 3A) even after accounting for the normal developmental increase in SP-D seen in WT animals. Neither Pale ear nor Pearl single mutation animals exhibited increases in BAL SP-D (data not shown). The magnitude of the difference in total SP-D between WT and EPPE animals increased with age, reaching nearly fourfold by 16 weeks (Figure 3B). This is in contrast to our prior report, in which we did not find differences in large and small aggregate total SP-D levels in comparing WT and EPPE animals at 16 weeks of age (7). In the present study we used an antibody with higher specificity for mouse (and human) SP-D (as described in the online supplement), and analyzed equal volumes of unfractionated BAL for total SP-D (4, 7). By comparison, SP-A levels were not elevated in the BAL of EPPE animals (data not shown).

We next examined BAL specimens for the presence of SP-D modifications. When controlled for input SP-D (Figure 4A, *bottom*), BAL from 2-week EPPE animals exhibited a fourfold increase in S-nitrosylated SP-D (SNO-SP-D) that increased further with age (Figure 4A, *top*). Increasing SNO-SP-D in EPPE animals was also associated with the presence of lower molecular weight forms of SP-D, evident by native gel electrophoresis of the BAL specimens (Figure 4A, *middle*), as we have previously demonstrated in other models of inflammation (9, 15). By contrast, BAL fluid from WT animals did not demonstrate disassembly of SP-D by native gel electrophoresis (2-wk WT as shown in Figure 4A; other ages not shown). SNO-SP-D formation was associated with increased NO production in EPPE mice as indicated by total NO in BAL fluid (data not shown). Increased production of nitrate relative to nitrite (Figure 4B) indicates that oxidative metabolism of NO predominates within EPPE mice.

Humans with HPS1 Exhibit Increased Alveolar SP-D and SNO-SP-D in Relation to Disease Severity

Seven patients with HPS1 were categorized as having minimal to mild disease (n = 3; FVC, 90 ± 9%; diffusing capacity of carbon

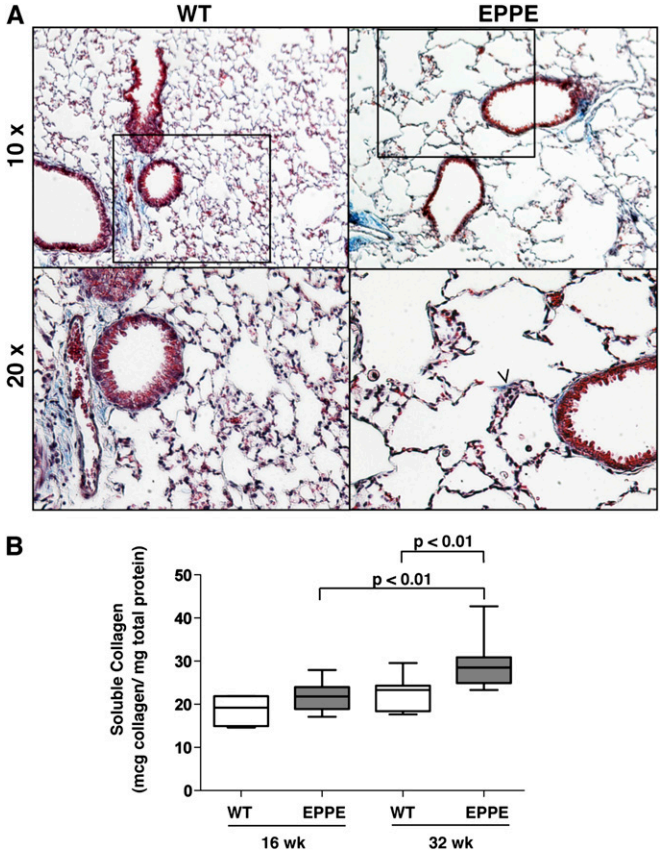

Figure 2. Ontogeny of pulmonary fibrosis in the pale ear/pearl (EPPE) model of Hermansky-Pudlak syndrome. (*A*) Wild-type (WT) and EPPE lungs were examined after inflation fixation, paraffin sectioning, and trichrome staining (n = 3 animals per age, genotype). Shown is a representative set of photomicrographs from 32-week WT and EPPE animals at an original magnification of ×10 (*top*) and ×20 (*bottom*). The frames in the *top panels* indicate the images illustrated in the *bottom panels*. *Blue staining* indicating collagen deposition is readily seen in the EPPE lung only at 32 weeks of age (*arrowhead*). (*B*) Soluble collagen as determined by the Sircol assay in lung tissue from WT and EPPE animals at 16 and 32 weeks of age (n = 7 or 8 animals per group, one-way analysis of variance).

monoxide [D_{LCO}], 77 ± 8%) or moderate to severe disease (n = 4; FVC, 59 ± 5%; D_{LCO}, 59 ± 13%) on the basis of pulmonary function testing performed at the time of bronchoscopy. Four normal volunteers similarly underwent bronchoscopy and pulmonary function testing for comparison (FVC, 103 ± 10%; D_{LCO}, 98 ± 10%). In aggregate, there was a trend toward increased total SP-D in patients with minimal/mild HPS1 disease, whereas the increase in patients with moderate/severe disease compared with normal volunteers reached statistical significance (Figures 5A and 5B). By comparison, SP-A levels were not elevated in the BAL of patients with HPS1 (data not shown). SNO-SP-D and lower molecular weight forms of SP-D on native gel electrophoresis were elevated in all patients with HPS1 (Figure 5C). In aggregate, there was a trend toward increased SNO-SP-D levels in the BAL from patients with minimal/mild HPS1 disease compared with normal volunteers, whereas SNO-SP-D levels were significantly elevated in BAL samples from patients with HPS1 with moderate/severe disease (Figure 5D).

Alveolar Type 2 Cells from EPPE Animals Produce Chemoattractant Cytokines

Enhanced local nitric oxide production is a primary mechanism for protein S-nitrosylation (22). This has been demonstrated for S-nitrosylation of SP-D as well (9), typically by activated macrophages in animal models of inflammation (23) although also more recently in humans (24). Although S-nitrosylated SP-D has been shown to be chemotactic for macrophages (9), our data indicate that SNO-SP-D was elevated before the infiltration of macrophages into the lungs of EPPE mice (Figure 1B), suggesting that other chemokines may be important in the early inflammatory response. There was a trend toward increased BAL JE, the mouse homolog of macrophage chemotactic protein-1 (subsequently referred to as MCP-1, also known as Ccl2), as early as 1 week postnatal age in EPPE mice, whereas other chemokines such as IL-12p40 were not elevated through 4 weeks of age in the EPPE mice (Figure 6A). This raised the possibility that alveolar type 2 cells, known to produce MCP-1 and nitric oxide synthase-2 (NOS2) in association with inflammation and injury (25–31), contribute to macrophage migration and local nitric oxide production in HPS. To test this, we collected BAL cells and isolated alveolar epithelial cells from 2- and 4-week animals as described in the online supplement. RT-PCR showed that epithelial cells were the primary source of MCP-1 in EPPE mice (average C_t for EPPE epithelial cells, 27.4 ± 2.9; Figure 6B). By contrast, alveolar epithelial cell expression of IL-12p40 was undetectable in WT and EPPE animals, and increased BAL cell expression of IL-12p40 was increased in EPPE cells over WT only in 4-week animals. Immunostaining of EPPE alveolar epithelial cells, after 4 hours

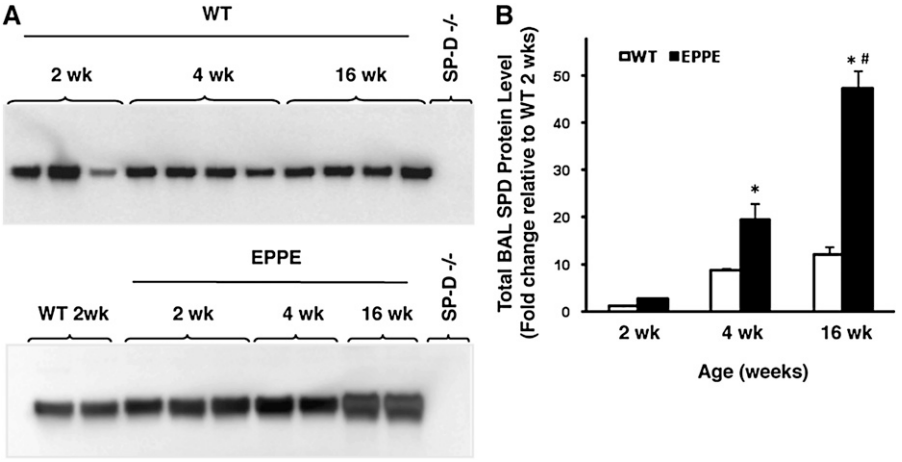

Figure 3. EPPE (pale ear/pearl) mice exhibit an increase in bronchoalveolar lavage (BAL) surfactant protein D (SP-D) levels. (*A*) Equal volumes of BAL from wild-type (WT) and EPPE mice at 2, 4, and 16 weeks of age were analyzed for total SP-D by sodium dodecyl sulfate–polyacrylamide gel electrophoresis, under reduced conditions followed by Western immunoblotting with anti–SP-D antibody. Data shown are representative of three independent experiments (n = 5 in each group). (*B*) Quantification of SP-D content as described in METHODS. *Open columns*, WT mice; *solid columns*, EPPE mice. *$P < 0.05$ versus 2-week WT level; #$P < 0.05$ versus WT at corresponding age, using one-way analysis of variance.

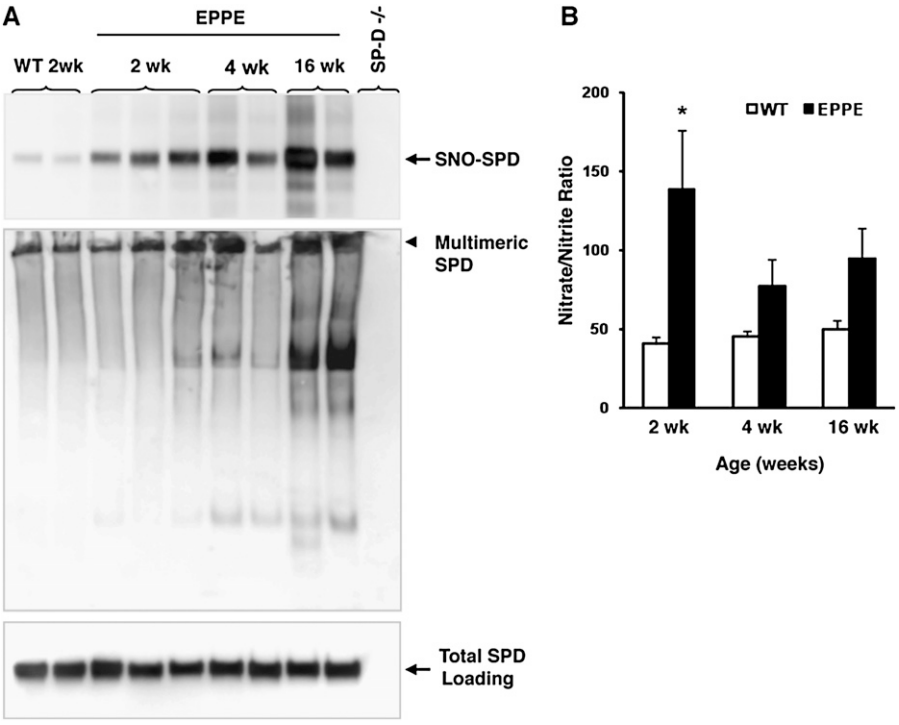

Figure 4. EPPE (pale ear/pearl) animals exhibit S-nitrosylation of surfactant protein D (SP-D) and altered SP-D quaternary structure. (*A*) Bronchoalveolar lavage (BAL) containing equal amounts of total SP-D (described in the online supplement and shown at *bottom*) from wild-type (WT) and EPPE mice at various ages was analyzed for S-nitrosylated SP-D (SNO-SP-D) content by the biotin-switch method. Data shown are representative of two separate analyses for each group (n = 5 animals per age, genotype). SNO-SP-D formation consistently increased with age in EPPE animals (*A, top*). BAL containing equal amounts of total SP-D (*A, bottom*) was subjected to native gel electrophoresis to determine the quaternary structure of SP-D (*A, middle*). Data shown are representative of two independent experiments (n = 5 animals per age, genotype). BAL from SP-D–deficient mice ($SP\text{-}D^{-/-}$) was included as a negative control. Multimeric SP-D is incapable of entering the gel at the top, whereas lower molecular weight forms are seen only in BAL from EPPE mice. (*B*) BAL samples from WT and EPPE mice at 2, 4, and 16 weeks of age were analyzed for total NO metabolites and NO_2^- as described in METHODS, and the data are expressed as the nitrate/nitrite ratio (n = 5; mean ± SEM; $^*P < 0.05$ vs. WT at corresponding age, using one-way analysis of variance).

of brefeldin A exposure to inhibit cytokine secretion, localized production of MCP-1 to ABCA3-positive alveolar type 2 cells (Figure 7).

To determine the source of NO production for the formation of SNO-SP-D, we examined alveolar epithelial cells and BAL cells for NOS2 expression by RT-PCR. Alveolar epithelial cells from 2- and 4-week-old EPPE mice expressed more NOS2 RNA (average C_t for EPPE epithelial cells, 29.5 ± 1.2 cycles) than WT epithelial cells and than WT and EPPE BAL cells (Figure 6C). Together these data indicate that alveolar epithelial cells produce the inflammatory mediators MCP-1 and NOS2 early in HPS lung disease in EPPE animals.

S-Nitrosylated SP-D in Animals and Patients with HPS Enhances Macrophage Migration together with MCP-1

We have previously shown that S-nitrosylated SP-D induces inflammatory cell activation (9). To test whether the SNO-SP-D or MCP-1 from EPPE animals or patients with HPS1 could be responsible for the increasing macrophage-predominant inflammation, we performed migration assays using the macrophage cell line RAW 264.7, and BAL from EPPE mice (Figure 8A) or patients with HPS1 (Figure 8B). BAL from 4-week WT animals did not increase cellular migration above control (defined as random migration toward culture medium). Chemically S-nitrosylated BAL fluid from WT animals (BAL-SNO) resulted in increased cell migration. By comparison, BAL from EPPE mice exhibited a nearly threefold increase in RAW cell migration compared with BAL-SNO. Pre-incubation of EPPE BAL with ascorbate to reduce *S*-nitrosothiols or with antibody directed against SP-D each decreased migration by more than 60%. Preincubation of RAW cells with antibody directed against CD91, a receptor for SNO-SP-D interactions (9), also reduced migration by more than 60%. Last, preincubation of EPPE BAL with MCP-1 antibody reduced migration by nearly 50% alone, and resulted in a further reduction of migration when combined with anti–SP-D.

Migration experiments were repeated with pooled BAL from patients with moderate to severe HPS1. S-nitrosylation of BAL from normal volunteers (NV-SNO) resulted in increased migration compared with unmodified BAL (NV). Pretreatment of NV-SNO BAL with ascorbate or anti–SP-D decreased migration to levels seen in unmodified NV BAL, and there was no effect of pretreatment with anti–MCP-1 on NV-SNO BAL. By contrast, BAL from patients with HPS1 with moderate–severe fibrosis elicited greater than twofold enhanced migration compared with NV-SNO. Migration in response to HPS1 BAL was reduced by pretreating HPS1 BAL with ascorbate, anti–SP-D, or anti–MCP-1, whereas migration was not affected by pretreating with normal mouse IgG. Combining anti–SP-D and anti–MCP-1 in the pretreatment of HPS1 BAL reduced the migration of RAW cells to levels comparable to unmodified BAL from normal volunteers.

DISCUSSION

Hermansky-Pudlak syndrome is a devastating multisystem disease afflicting roughly 1,000 patients worldwide but especially 1 in 1,800 inhabitants of Puerto Rico, caused by a genetic mutation in the HPS1 gene that has propagated in the population through a founder effect (32). Pulmonary findings commonly described in adults with HPS from case series and case reports include macrophage-predominant inflammation, ceroid deposits within macrophages, and progressive honeycombing on high-resolution computed tomography indicative of progressive pulmonary fibrosis (3, 33, 34). Longitudinal studies establishing the natural history of HPS lung disease are limited and have included only adults after presentation with restrictive lung remodeling. With this in mind, we sought to improve our understanding of the pulmonary disease pathogenesis in HPS through the use of an animal model, specifically to identify early events and their molecular basis.

Our first objective was to describe the ontogeny of lung disease in the pale ear/pearl (EPPE) mouse model, a model characterized by others as spontaneously developing fibrotic lung remodeling (8). The EPPE mouse model, a cross between two HPS mouse strains, was developed previously to facilitate

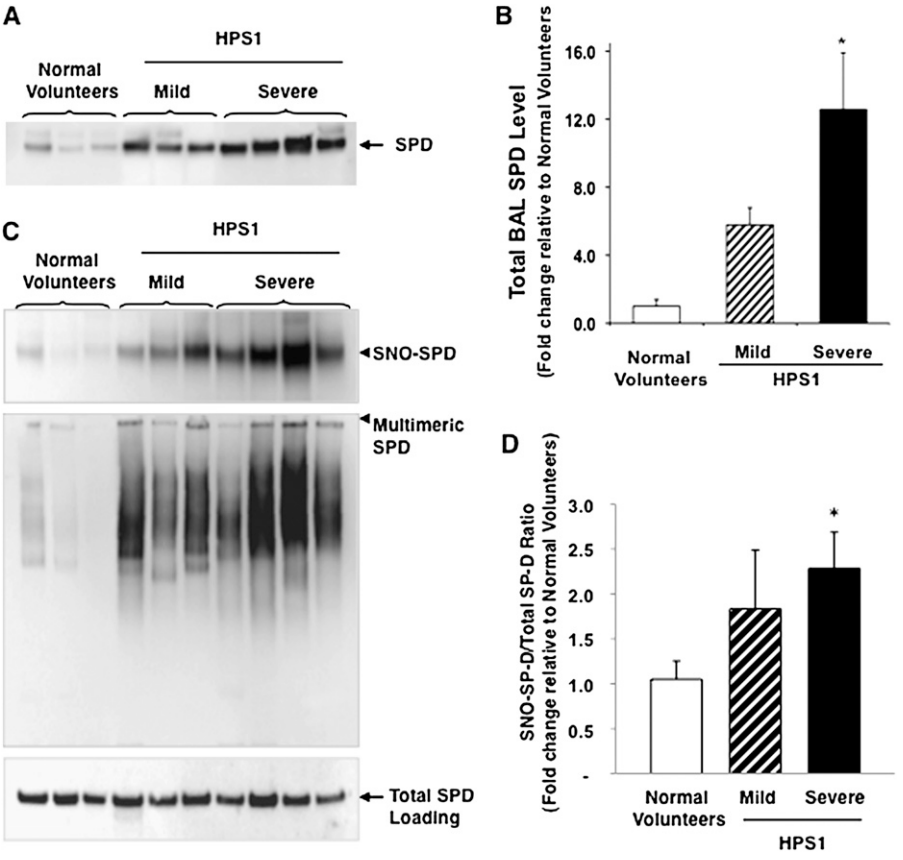

Figure 5. Surfactant protein D (SP-D) modifications and structure disruption occur in human Hermansky-Pudlak syndrome type 1 (HPS1) pulmonary fibrosis and are associated with disease severity. (*A*) Equal volumes of bronchoalveolar lavage (BAL) fluid from healthy volunteers and patients with HPS1 were analyzed for total SP-D by sodium dodecyl sulfate–polyacrylamide gel electrophoresis, under reduced conditions followed by Western immunoblotting with anti–SP-D antibody. (*B*) Quantification of total SP-D content. Data are expressed as fold increase compared with normal volunteer samples. *Open column*, normal volunteers (n = 4); *hatched column*, patients with HPS1 with minimal to mild lung disease (n = 3); *solid column*, patients with HPS1 with moderate to severe disease (n = 4). (*C*) BAL containing equal amounts of total SP-D (described in the online supplement and shown at *bottom*) were analyzed for S-nitrosylated SP-D (SNO-SP-D) content by the biotin-switch method. Increases in SNO-SP-D formation were associated with increased disease severity (*C*, *top*). BAL containing equal amounts of total SP-D was subjected to native gel electrophoresis to determine the quaternary structure of SP-D (*C*, *middle*). (*D*) Quantification of SNO-SP-D content. Data are expressed as the ratio of S-nitrosylated SP-D over total SP-D, and represented as fold change relative to normal volunteers. *Open column*, normal volunteers (n = 4); *hatched column*, patients with HPS1 with mild lung disease (n = 3); *solid column*, patients with HPS1 with severe pulmonary fibrosis (n = 4). *$P < 0.05$ versus normal volunteers, using one-way analysis of variance.

studies of HPS lung disease (4). The pale ear and pearl parent strains, although demonstrating lamellar body enlargement and an inflammatory cell infiltrate, did not develop fibrosis unless challenged with bleomycin (6). Single-mutation animals exhibited increased susceptibility to LPS challenge with more exuberant cytokine responses (5). Although macrophages from adult pale ear or pearl animals exhibited some evidence of activation, specifically increased tumor necrosis factor-α and IL-12p40, it was attributed to an abnormal alveolar milieu because these macrophages rapidly became quiescent when cultured *in vitro*, and cell-free BAL from these animals was able to activate otherwise normal alveolar macrophages.

The advantage of the EPPE mouse model is that it recapitulates all the features of adult HPS lung disease with the presence of giant lamellar bodies in alveolar epithelial cells, inflammation, and lung remodeling including fibrosis, albeit also in the context of airspace enlargement not reported in human HPS (4, 8). The present study uses this animal model to establish the temporal relationships between each facet of the disease. We have demonstrated a reproducible ontogeny for the onset of HPS lung disease in EPPE mice that begins with lamellar body enlargement and tissue phospholipid accumulation followed by alveolar inflammation, with these events being separated by up to 4 weeks and with each increasing in severity into adulthood. Furthermore, alveolar inflammation precedes lung remodeling, consisting of both airspace enlargement and subsequent collagen deposition (8). Our longitudinal survey demonstrated that alveolitis began much earlier than previously suggested by BAL studies in both HPS mouse models carrying single mutations, and adult patients with HPS1 (14, 34, 35). These data provide strong support for a more comprehensive evaluation of the pediatric HPS population, and suggest that earlier treatment protocols (before the development of clinically apparent restrictive lung disease) may be important in modifying the disease course.

Our longitudinal studies uncovered an interesting period in the natural history of HPS in the EPPE mouse. We identified a period during which there is evidence of a growing aberrant type 2 cell phenotype signified by lamellar body distention, increasing tissue phospholipid deposition, and type 2 cell hyperplasia, which precedes the initiation of the macrophage-predominant alveolar infiltrate. Thus, the second objective of our study was to explore this period for potential disease mechanisms. There has been increasing evidence that epithelial cell injury is an important factor in the development of HPS lung disease. Both Mahavadi and colleagues (8) and Young and colleagues (6) have reported evidence of epithelial cell injury, and prior work by Young and colleagues (5) suggests that the alveolar inflammation is a reactive and not a primary feature of HPS. Our data strongly support the alveolar type 2 cell as the initiator of lung disease in HPS. Isolated type 2 cells from EPPE mice as early as 2 weeks of age exhibit a proinflammatory phenotype with the production of at least two molecular mediators, specifically MCP-1 and inducible nitric oxide synthase (iNOS). Although it is likely that other cytokines and chemokines are produced by the alveolar epithelium from EPPE animals, our studies indicate that together MCP-1 and SNO-SP-D contribute the majority of the chemotactic activity in the alveolar space early in HPS lung disease, accounting for up to 75% of the chemotaxis induced by EPPE mouse BAL as early as 4 weeks of age. Although MCP-1 production by alveolar macrophages may play a more prominent role in macrophage activation with

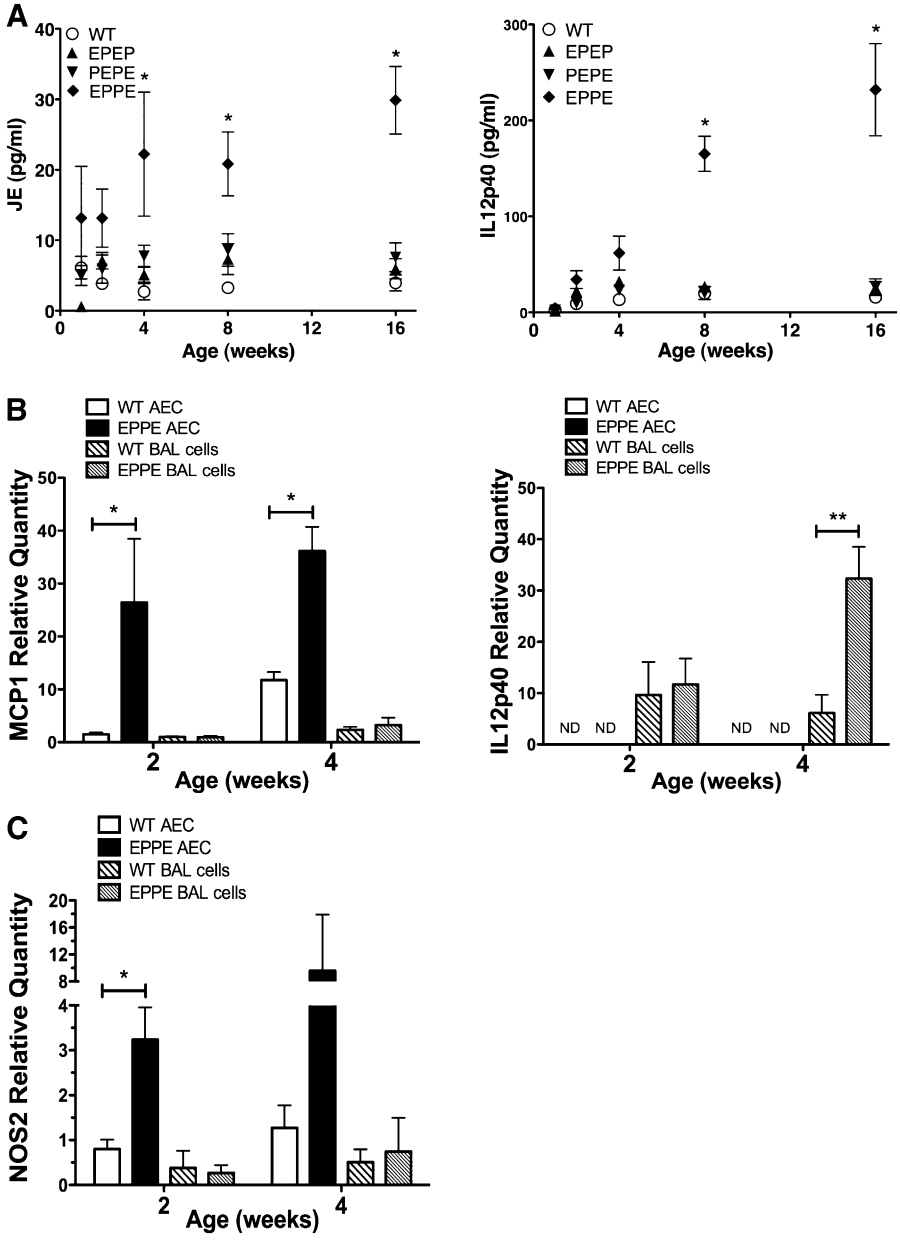

Figure 6. Alveolar epithelial cells (AECs) contribute to early inflammation in animal models of Hermansky-Pudlak syndrome. (*A*) Bronchoalveolar lavage (BAL) samples were assayed for JE, the mouse homolog of macrophage chemotactic protein-1 (MCP-1), and IL-12p40, using a Searchlight multiplex format (n = 2–6 samples; samples from animals ⩽ 2 wk represent pools of 2–4 animals). Data are shown as concentrations (pg/ml) and were analyzed by two-way analysis of variance (ANOVA) (*$P < 0.05$ vs. wild-type [WT] at corresponding age). (*B*) Relative real-time polymerase chain reaction (PCR) for MCP-1 and IL-12p40 was performed from AECs or BAL cells isolated from WT and EPPE animals at 2 and 4 weeks of age (ND, none detected; *$P < 0.05$ vs. WT AECs at corresponding age, **$P < 0.01$ vs. WT BAL cells at corresponding age by two-way ANOVA). (*C*) Relative real-time PCR for nitric oxide synthase-2 (NOS2) performed from AECs or BAL cells isolated from WT and EPPE animals at 2 and 4 weeks of age (ND, none detected; *$P < 0.05$ vs. WT alveolar type 2 [AT2] cells at corresponding age by one-way ANOVA). EPEP = pale ear; EPPE = pale ear/pearl; PEPE = pearl.

advanced disease in patients with HPS1 (14), our data are the first to suggest that the alveolar epithelium may play a prominent role in elaborating inflammatory mediators early in HPS disease.

Whereas MCP-1 has clearly been linked to the pathogenesis of HPS lung disease in studies of patients with HPS1 (14), our data establish the importance of SP-D in the pathogenesis of HPS lung disease in both mice and humans. SP-D has emerged as a key modulator of inflammation in the alveolar space (36). In its multimeric form, the lectin-binding domains interact with surface receptors such as SIRPα on effector cells, attenuating NF-κB–mediated proinflammatory gene expression (37). In a variety of models of pulmonary inflammation using exogenous inflammatory stimuli (bleomycin, *Pneumocystis*), we have shown previously that alveolar inflammation leads to local production of NO metabolites via increased iNOS expression by activated macrophages, promoting S-nitrosylation of SP-D and disrupting SP-D tertiary structure (9, 15). Studies of patients with asthma similarly show that SNO-SP-D was associated with pulmonary inflammation and was predictive of response to segmental allergen challenges (24), expanding the usefulness of SNO-SP-D as a biomarker of inflammation. The mechanism by which SNO-SP-D promotes a proinflammatory state stems from trimeric SNO-SP-D having accessibility to surface receptors, such as CD91, that trigger proinflammatory responses such as macrophage migration and induction of iNOS (9). This signaling pathway, which is highly sensitive to small amounts of SNO-SP-D, is not otherwise accessible to multimeric SP-D (9). By contrast, oxidized SP-D, which results in cross-linking of SP-D, results in inactivation of LPS agglutination by SP-D (38) and does not stimulate inflammatory responses (24).

Our initial studies of the EPPE mouse model (7), in which we characterized surfactant abnormalities in adult mice but did not demonstrate differences in SP-D, highlight an important issue. It is becoming clear from animal models and human studies that the complex oligomeric structure of SP-D and its liability for disruption in disease models call for a comprehensive analysis of SP-D (36). The availability of new antisera (39) with better specificity for murine and human SP-D than we used previously, and the advent of new techniques including the

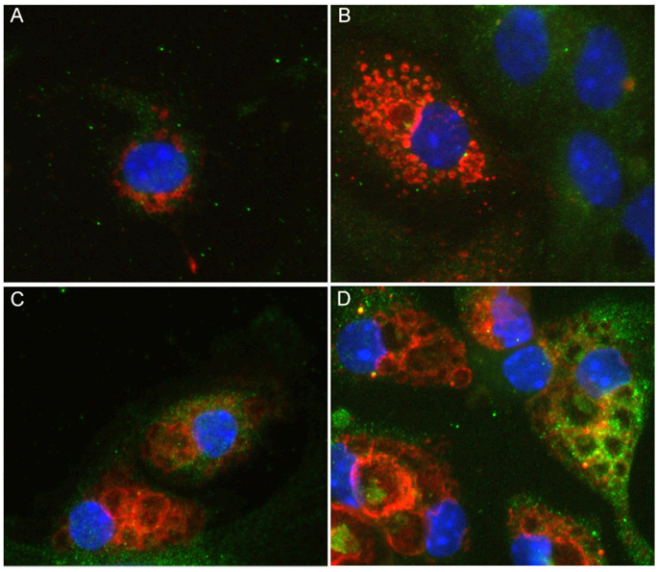

Figure 7. Alveolar type 2 (AT2) cells from animal models of Hermansky-Pudlak syndrome produce monocyte chemotactic protein-1 (MCP-1). Representative photomicrographs of isolated alveolar epithelial cells from 2-week (*A* and *C*) and 4-week (*B* and *D*), wild-type (WT) (*A* and *B*) and EPPE (pale ear/pearl) (*C* and *D*) animals treated with brefeldin for 4 hours (n = 3 experiments each in which AT2 cells were derived from four animals). Samples were examined for the presence of ABCA3 (*red*; 3c9 antibody) as a marker of AT2 cells and for the presence of MCP-1 (*green*). 4′,6-Diamidino-2-phenylindole was used to counterstain nuclei (*blue*).

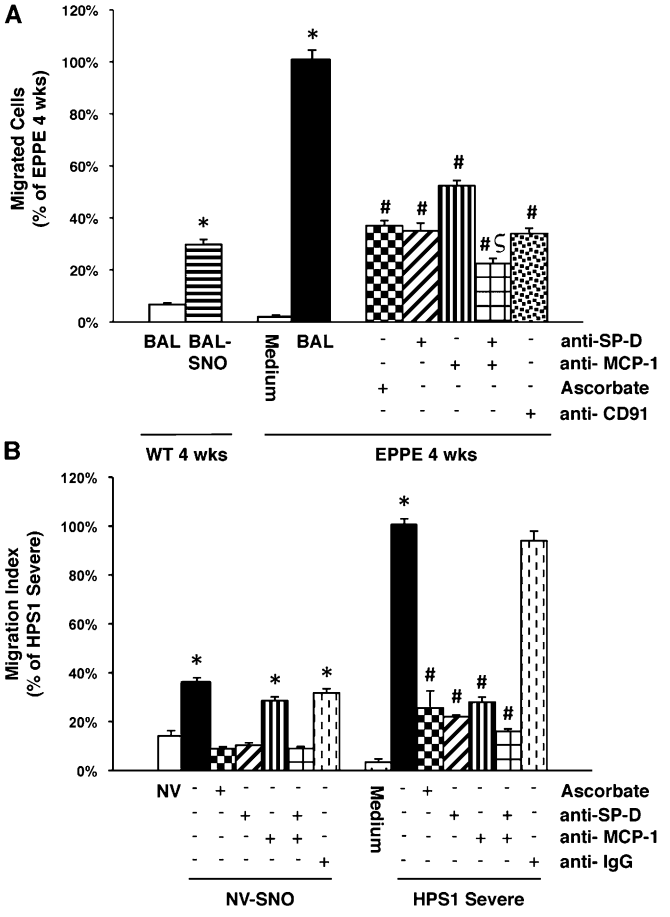

Figure 8. Hermansky-Pudlak syndrome type 1 (HPS1) bronchoalveolar lavage (BAL) induces macrophage chemotaxis in part through S-nitrosylated surfactant protein D (SNO-SP-D). BAL from 4-week-old wild-type (WT) and pale ear/pearl (EPPE) mice was assayed for the ability to induce RAW 264.7 macrophage migration, using a modified Boyden chamber as described in METHODS. Briefly, suspensions of RAW 264.7 cells (2×10^6 cells/ml in Dulbecco's modified Eagle's medium) were allowed to migrate toward BAL fluid from 4-week-old WT versus EPPE mice (*A*), or normal volunteers (NV) versus patients with HPS1 (*B*) for 3 hours with 5% CO_2 at 37°C. Basal migration was expressed as the numbers of cells migrating toward medium only. Positive controls consisted of samples exposed to L-S-nitrosocysteine (L-SNOC) (200 mM) to S-nitrosylate all available proteins from 4-week-old WT (BAL SNO) or NV (NV-SNO). Samples of BAL were also pretreated overnight with anti–SP-D (20 mg/ml) ± anti–MCP-1 (20 mg/ml) antibody followed by immunoprecipitation before adding sample to the Boyden chamber. The importance of SNO-SP-D to chemotaxis was demonstrated by pretreatment of RAW 264.7 cells with anti-CD91 antibody (20 mg/ml) or 20 mM ascorbic acid for 20 minutes before exposure to BAL. Data are normalized as the percentage of cells migrated toward BAL of 4-week EPPE mice (*A*: $^*P < 0.05$ vs. 4-wk WT mice; $^{\#}P < 0.05$ vs. 4-wk EPPE mice; $^{\zeta}P < 0.05$ vs. pretreatment with MCP-1 antibody) or BAL of patients with HPS1 (*B*: $^*P < 0.05$ vs. NV; $^{\#}P < 0.05$ vs. patients with HPS1). All measurements were performed in triplicate and are representative of three independent experiments analyzed by one-way analysis of variance.

biotin-switch assay to detect S-nitrosyl protein modifications and native gel electrophoresis to examine the quaternary structure of SP-D, enabled us to revisit the role of SP-D in HPS. In the current study, we found both increases in total SP-D and SNO-SP-D in HPS BAL from both EPPE mice and patients with HPS1. In our prior study we normalized total SP-D immunoblotting data to BAL total protein and total phospholipid. This normalization presented a problem in retrospect because of elevated total protein and reduced total phospholipid in BAL from EPPE mice, as we and others have reported (4, 7), leading us to conclude that total SP-D was not altered in the EPPE mice. In the present study we instead reported total SP-D in equivalent volumes of BAL from EPPE mice (Figure 3) and patients with HPS1 (Figure 5), and found dramatic differences that progressed with age in EPPE mice, and with disease severity in patients with HPS1. In examining SNO-SP-D and changes in quaternary structure, we instead started with samples containing equal amounts of total SP-D, so that the analysis was not confounded by the already increased SP-D in BAL from EPPE mice and patients with HPS1. Together, this more thorough examination in both the EPPE mouse and patients with HPS1 has uncovered an important role for SNO-SP-D as an amplifier of inflammation in HPS lung disease.

The effects of SNO-SP-D in EPPE mice and patients with HPS1 are reminiscent of our prior studies in bleomycin-treated mice, in which enhanced chemotaxis *in vitro* due to BAL SNO-SP-D was mitigated by removal of *S*-nitrosothiols, using ascorbate or by immunodepletion SP-D (9). It is interesting that whereas SNO-SP-D has been shown to mediate both migration and activation of macrophages in response to bleomycin injury, in our current study the dominant effect of SNO-SP-D is on macrophage migration early in the pathogenesis of HPS lung disease in EPPE mice. Another interesting difference between our prior work using the bleomycin model and our current studies in EPPE animals relates to the source of NO. S-nitrosylation of proteins largely occurs in the context of increased NO production (22), which in the lung occurs typically from activated macrophages expressing iNOS (23). In bleomycin-treated animals, S-nitrosylation resulted from enhanced NO production via iNOS induced in alveolar macrophages (9). In young EPPE animals, the source of NO

production uncharacteristically arose from the alveolar epithelium. NO production from the induction of type 2 cell iNOS has been described previously in response to external inflammatory stimuli, in cell lines (29, 31) and with injury from bleomycin *in vivo* (30). In HPS lung disease, the stimulus is endogenous, possibly from pathways within alveolar type 2 cells activated in response to lamellar body enlargement.

The role of inflammation in the pathogenesis of pulmonary fibrosis has been controversial, with more recent evidence validating the central role of repetitive epithelial injury in fibroproliferation (40). Studies of type 2 cell–targeted expression of diphtheria toxin receptor suggest that not only epithelial injury but injury to important progenitor cells in the alveolus initiate fibroproliferation (41). Pulmonary fibrosis from overexpression of transforming growth factor (TGF)-β_1, using adenovirus, emphasizes the role of the epithelial–mesenchymal transition (EMT) to the process of fibroproliferation (42), and conditional overexpression of TGF-α now makes a strong case for non-EMT pathways in the process of pulmonary fibrosis (43). However, two of these models of fibrosis have similarly been associated with alveolar inflammation (44, 45). Thus, inflammation may simply be a proxy for alveolar epithelial injury, or may function as an amplifier of injury that contributes to the process of remodeling, as seen in acute exacerbations of idiopathic pulmonary fibrosis (46).

The data presented in this study point to a chronic, unremitting injury of alveolar epithelial cells in HPS, leading to the elaboration of proinflammatory mediators. Like others (6, 8), we are unable to determine from our present studies whether the observed inflammatory signals in EPPE animals directly contribute to the development of fibrosis in animal models of HPS, or are simply an earlier marker of a failing epithelial cell. Although inflammation may be a secondary manifestation of alveolar type 2 cell dysfunction, it represents a reliable early end point for future studies as well as a potential therapeutic target. Moreover, SNO-SP-D as a mediator of inflammation in HPS is an attractive candidate for a new biomarker in HPS lung disease that tracked well with disease progression in both the mouse model as well as in patients with HPS1. Taken together, these studies clarify the ontogeny of HPS lung disease in a reliable mouse model for future studies of disease pathogenesis and preclinical testing of therapeutic agents, and establish key mediators of the disease as well as a potential biomarker for expanded investigation in patients with HPS.

Author Disclosure: E.N.A.-V., S.R.B., P.Z., H.A., Z.Z., L.G., J.-Q.T., B.R.G., W.G., C.-J.G., A.J.G., and M.F.B. do not have a financial relationship with a commercial entity that has an interest in the subject of this manuscript. S.G. received lecture fees from Mead Johnson and Abbott Nutritionals, and received grant support from the American Heart Association.

Acknowledgment: The authors thank the patients who participated in this study for their contributions to this research, and greatly appreciate the continued support of Donna and Richard Appel and the HPS Network (www.hpsnetwork.org). The authors also thank Ping Wang for technical contributions in the preparation of isolated alveolar epithelial cells.

References

1. Huizing M, Helip-Wooley A, Westbroek W, Gunay-Aygun M, Gahl WA. Disorders of lysosome-related organelle biogenesis: clinical and molecular genetics. *Annu Rev Genomics Hum Genet* 2008;9:359–386.
2. Gochuico BR, Huizing M, Golas G, Gahl WA. Interstitial lung disease in Hermansky-Pudlak syndrome-2. *Am J Respir Crit Care Med* 2010;181: A6018.
3. Nakatani Y, Nakamura N, Sano J, Inayama Y, Kawano N, Yamanaka S, Miyagi Y, Nagashima Y, Ohbayashi C, Mizushima M, *et al*. Interstitial pneumonia in Hermansky-Pudlak syndrome: significance of florid foamy swelling/degeneration (giant lamellar body degeneration) of type-2 pneumocytes. *Virchows Arch* 2000;437:304–313.
4. Lyerla TA, Rusiniak ME, Borchers M, Jahreis G, Tan J, Ohtake P, Novak EK, Swank RT. Aberrant lung structure, composition, and function in a murine model of Hermansky-Pudlak syndrome. *Am J Physiol Lung Cell Mol Physiol* 2003;285:L643–L653.
5. Young LR, Borchers MT, Allen HL, Gibbons RS, McCormack FX. Lung-restricted macrophage activation in the *pearl* mouse model of Hermansky-Pudlak syndrome. *J Immunol* 2006;176:4361–4368.
6. Young LR, Pasula R, Gulleman PM, Deutsch GH, McCormack FX. Susceptibility of Hermansky-Pudlak mice to bleomycin-induced type II cell apoptosis and fibrosis. *Am J Respir Cell Mol Biol* 2007;37:67–74.
7. Guttentag SH, Akhtar A, Tao JQ, Atochina E, Rusiniak ME, Swank RT, Bates SR. Defective surfactant secretion in a mouse model of Hermansky-Pudlak syndrome. *Am J Respir Cell Mol Biol* 2005;33:14–21.
8. Mahavadi P, Korfei M, Henneke I, Liebisch G, Schmitz G, Gochuico BR, Markart P, Bellusci S, Seeger W, Ruppert C, *et al*. Epithelial stress and apoptosis underlie Hermansky-Pudlak syndrome–associated interstitial pneumonia. *Am J Respir Crit Care Med* 2010;182:207–219.
9. Guo CJ, Atochina-Vasserman EN, Abramova E, Foley JP, Zaman A, Crouch E, Beers MF, Savani RC, Gow AJ. S-nitrosylation of surfactant protein-D controls inflammatory function. *PLoS Biol* 2008;6:e266.
10. Atochina-Vasserman E, Abramova H, Zhang P, Gow AJ, Beers MF, Guttentag SH. Post-translational modifications of surfactant protein D (SP-D) in Hermansky-Pudlak syndrome [abstract]. *Am J Respir Crit Care Med* 2010;181:A2447.
11. Lowry OH, Rosebrough NJ, Farr AL, Randall RJ. Protein measurement with the Folin phenol reagent. *J Biol Chem* 1951;193:265–275.
12. Bligh EG, Dyer WJ. A rapid method of total lipid extraction and purification. *Can J Biochem Physiol* 1959;37:911–917.
13. Bartlett G. Phosphorus assay in column chromatography. *J Biol Chem* 1959;234:466.
14. Rouhani FN, Brantly ML, Markello TC, Helip-Wooley A, O'Brien K, Hess R, Huizing M, Gahl WA, Gochuico BR. Alveolar macrophage dysregulation in Hermansky-Pudlak syndrome type 1. *Am J Respir Crit Care Med* 2009;180:1114–1121.
15. Atochina-Vasserman EN, Gow AJ, Abramova H, Guo CJ, Tomer Y, Preston AM, Beck JM, Beers MF. Immune reconstitution during *Pneumocystis* lung infection: disruption of surfactant component expression and function by S-nitrosylation. *J Immunol* 2009;182:2277–2287.
16. Foster C, Aktar A, Kopf D, Zhang P, Guttentag S. Pepsinogen C: a type 2 cell–specific protease. *Am J Physiol Lung Cell Mol Physiol* 2004; 286:L382–L387.
17. Mahavadi P, Korfei M, Ruppert C, Seeger W, Guenther A. Evidence of surfactant accumulation and type II pneumocyte apoptosis in Hermansky Pudlak syndrome associated lung fibrosis. *Am J Respir Crit Care Med* 2008;177:A823.
18. Atochina EN, Beers MF, Scanlon ST, Preston AM, Beck JM. *P. carinii* induces selective alterations in component expression and biophysical activity of lung surfactant. *Am J Physiol Lung Cell Mol Physiol* 2000; 278:L599–L609.
19. Casey J, Kaplan J, Atochina-Vasserman EN, Gow AJ, Kadire H, Tomer Y, Fisher JH, Hawgood S, Savani RC, Beers MF. Alveolar surfactant protein D content modulates bleomycin-induced lung injury. *Am J Respir Crit Care Med* 2005;172:869–877.
20. Gardai SJ, Xiao YQ, Dickinson M, Nick JA, Voelker DR, Greene KE, Henson PM. By binding SIRPα or calreticulin/CD91, lung collectins act as dual function surveillance molecules to suppress or enhance inflammation. *Cell* 2003;115:13–23.
21. Jain D, Atochina-Vasserman EN, Tomer Y, Kadire H, Beers MF. Surfactant protein D protects against acute hyperoxic lung injury. *Am J Respir Crit Care Med* 2008;178:805–813.
22. Foster MW, Hess DT, Stamler JS. Protein S-nitrosylation in health and disease: a current perspective. *Trends Mol Med* 2009;15:391–404.
23. Gaston B, Drazen JM, Loscalzo J, Stamler JS. The biology of nitrogen oxides in the airways. *Am J Respir Crit Care Med* 1994;149:538–551.
24. Atochina-Vasserman EN, Winkler C, Abramova H, Beers MF, Schaumann F, Krug N, Gow AJ, Hohlfeld JM. Segmental allergen challenge produces alterations in expression, multimeric structure, and function of surfactant protein D in humans. *Am J Respir Crit Care Med* 2011;183:856–864.
25. Antoniades HN, Neville-Golden J, Galanopoulos T, Kradin RL, Valente AJ, Graves DT. Expression of monocyte chemoattractant protein 1

mRNA in human idiopathic pulmonary fibrosis. *Proc Natl Acad Sci USA* 1992;89:5371–5375.
26. Moore BB, Peters-Golden M, Christensen PJ, Lama V, Kuziel WA, Paine R III, Toews GB. Alveolar epithelial cell inhibition of fibroblast proliferation is regulated by MCP-1/CCR2 and mediated by PGE_2. *Am J Physiol Lung Cell Mol Physiol* 2003;284:L342–L349.
27. Standiford TJ, Kunkel SL, Phan SH, Rollins BJ, Strieter RM. Alveolar macrophage–derived cytokines induce monocyte chemoattractant protein-1 expression from human pulmonary type II–like epithelial cells. *J Biol Chem* 1991;266:9912–9918.
28. Wang H, Yi T, Zheng Y, He S. Induction of monocyte chemoattractant protein-1 release from A549 cells by agonists of protease-activated receptor-1 and -2. *Eur J Cell Biol* 2007;86:233–242.
29. Hoyt JC, Ballering J, Numanami H, Hayden JM, Robbins RA. Doxycycline modulates nitric oxide production in murine lung epithelial cells. *J Immunol* 2006;176:567–572.
30. Inghilleri S, Morbini P, Oggionni T, Barni S, Fenoglio C. *In situ* assessment of oxidant and nitrogenic stress in bleomycin pulmonary fibrosis. *Histochem Cell Biol* 2006;125:661–669.
31. Korhonen R, Linker K, Pautz A, Forstermann U, Moilanen E, Kleinert H. Post-transcriptional regulation of human inducible nitric-oxide synthase expression by the Jun N-terminal kinase. *Mol Pharmacol* 2007;71:1427–1434.
32. Santiago Borrero PJ, Rodriguez-Perez Y, Renta JY, Izquierdo NJ, Del Fierro L, Munoz D, Molina NL, Ramirez S, Pagan-Mercado G, Ortiz I, *et al*. Genetic testing for oculocutaneous albinism type 1 and 2 and Hermansky-Pudlak syndrome type 1 and 3 mutations in Puerto Rico. *J Invest Dermatol* 2006;126:85–90.
33. Brantly M, Avila NA, Shotelersuk V, Lucero C, Huizing M, Gahl WA. Pulmonary function and high-resolution CT findings in patients with an inherited form of pulmonary fibrosis, Hermansky-Pudlak syndrome, due to mutations in HPS-1. *Chest* 2000;117:129–136.
34. Takahashi K, Ishida T, Ogura G, Ishii T, Oshima K, Sato S, Muroi M, Kanazawa K, Saito J, Otsuka Y, *et al*. Diagnostic usefulness of bronchoalveolar lavage in Hermansky-Pudlak syndrome: a case with double lung cancers. *Intern Med* 2004;43:972–976.
35. White DA, Smith GJ, Cooper JA Jr, Glickstein M, Rankin JA. Hermansky-Pudlak syndrome and interstitial lung disease: report of a case with lavage findings. *Am Rev Respir Dis* 1984;130:138–141.
36. Atochina-Vasserman EN, Beers MF, Gow AJ. Review: chemical and structural modifications of pulmonary collectins and their functional consequences. *Innate Immun* 2010;16:175–182.
37. Chroneos ZC, Sever-Chroneos Z, Shepherd VL. Pulmonary surfactant: an immunological perspective. *Cell Physiol Biochem* 2008;25:13–26.
38. Matalon S, Shrestha K, Kirk M, Waldheuser S, McDonald B, Smith K, Gao Z, Belaaouaj A, Crouch EC. Modification of surfactant protein D by reactive oxygen–nitrogen intermediates is accompanied by loss of aggregating activity, *in vitro* and *in vivo*. *FASEB J* 2009;23:1415–1430.
39. Atochina EN, Beck JM, Preston AM, Haczku A, Tomer Y, Scanlon ST, Fusaro T, Casey J, Hawgood S, Gow AJ, *et al*. Enhanced lung injury and delayed clearance of *Pneumocystis carinii* in surfactant protein A–deficient mice: attenuation of cytokine responses and reactive oxygen–nitrogen species. *Infect Immun* 2004;72:6002–6011.
40. Selman M, Pardo A. Role of epithelial cells in idiopathic pulmonary fibrosis: from innocent targets to serial killers. *Proc Am Thorac Soc* 2006;3:364–372.
41. Sisson TH, Mendez M, Choi K, Subbotina N, Courey A, Cunningham A, Dave A, Engelhardt JF, Liu X, White ES, *et al*. Targeted injury of type II alveolar epithelial cells induces pulmonary fibrosis. *Am J Respir Crit Care Med* 2010;181:254–263.
42. Kim KK, Wei Y, Szekeres C, Kugler MC, Wolters PJ, Hill ML, Frank JA, Brumwell AN, Wheeler SE, Kreidberg JA, *et al*. Epithelial cell $\alpha_3\beta_1$ integrin links β-catenin and Smad signaling to promote myofibroblast formation and pulmonary fibrosis. *J Clin Invest* 2009;119:213–224.
43. Hardie WD, Hagood JS, Dave V, Perl AK, Whitsett JA, Korfhagen TR, Glasser S. Signaling pathways in the epithelial origins of pulmonary fibrosis. *Cell Cycle* 2010;9:2769–2776.
44. Osterholzer JJ, Chen G-H, Lin Y, Subbotina N, Sisson TH. Targeted type II alveolar epithelial cell injury induced pulmonary fibrosis causes inflammation enriched for $Cd11b^+$ dendritic cells and exudate macrophages. *Am J Respir Crit Care Med* 2011;183:A6148.
45. Bonniaud P, Kolb M, Galt T, Robertson J, Robbins C, Stampfli M, Lavery C, Margetts PJ, Roberts AB, Gauldie J. Smad3 null mice develop airspace enlargement and are resistant to TGF-β–mediated pulmonary fibrosis. *J Immunol* 2004;173:2099–2108.
46. Kim DS, Park JH, Park BK, Lee JS, Nicholson AG, Colby T. Acute exacerbation of idiopathic pulmonary fibrosis: frequency and clinical features. *Eur Respir J* 2006;27:143–150.